

# The Green Synthesis of Silver Oxide Nanoparticles and Chitosan-Based on Silver Oxide Nanocomposite for Targeted Treatment of Invitro Anti Diabetic Activity

<sup>1</sup>Mugila Sinduja. S, <sup>2</sup>Ragel Mabel Saroja. R

<sup>1</sup>Mugila Sinduja. S, Research Scholar (Reg. No. 21113162032012), Department of Chemistry and Research Centre Scott Christian College (Autonomous), Nagercoil-629003, Affiliated to Manonmaniam Sundaranar University, Abishekapatti, Tirunelveli – 627 012, Tamilnadu, India.

<sup>2</sup>Ragel Mabel Saroja. R, Associate Professor, Department of Chemistry and Research Centre Scott Christian College (Autonomous), Nagercoil-629003, Affiliated to Manonmaniam Sundaranar University, Abishekapatti, Tirunelveli – 627 012, Tamilnadu, India.

Corresponding Author E-mail: [ragelmabelsaroja@yahoo.co.in](mailto:ragelmabelsaroja@yahoo.co.in)

---

Cite this paper as: Mugila Sinduja. S, Ragel Mabel Saroja. R (2024) The Green Synthesis of Silver Oxide Nanoparticles and Chitosan-Based on Silver Oxide Nanocomposite for Targeted Treatment of Invitro Anti Diabetic Activity. *Frontiers in Health Informatics*, 13 (4), 1641-1651

---

## Abstract

This study aimed to evaluate and compare the anti-diabetic effects of silver oxide nanoparticles (Ag<sub>2</sub>ONPs) and chitosan-silver oxide nanocomposite (CS-Ag<sub>2</sub>O NC). The nanoparticles and nanocomposite were made using a green synthesis technique, and their anti-diabetic activities were evaluated using in vitro models. The results showed that the CS-Ag<sub>2</sub>O nanocomposite had a stronger anti-diabetic effect than Ag<sub>2</sub>ONPs due to improved glucose absorption, insulin sensitivity, and alpha-glucosidase inhibition. The nanocomposite also showed reduced toxicity and improved biocompatibility. The study concludes that CS-Ag<sub>2</sub>O NC exhibits potential as a material for the development of anti-diabetic drugs. Infrared spectroscopy (FTIR), X-ray diffraction (XRD), EDAX analysis, and UV-vis spectroscopy were used to characterise the nanoparticles and nanocomposite. According to the findings, CS-Ag<sub>2</sub>O NC and significant Ag<sub>2</sub>ONPs had great anti-diabetic potential.

## Highlight

- Exhibits anti-diabetic activity in vitro and in vivo.
- Improves biocompatibility and stability.
- Modulates glucose metabolism and insulin signaling.
- Potential therapeutic application for diabetes treatment.
- Demonstrates enhanced efficacy with chitosan nanocomposites.

**Key words-** *Azadirachta Indica* biosynthesis anti-diabetic, nanocomposite, nanoparticles.

## 1. Introduction

Nanotechnology is a fast-evolving field of research in contemporary science and technology due to its many applications in physical, chemical, and biological systems that significantly affect the nation's economy and culture [1]. Metal nanoparticles' unique characteristics, such as their conductivity, transparency, catalysis, and magnetic properties, give them a wide range of uses.

Numerous physical and chemical techniques [2][3] have been developed for the creation of nanoparticles, but most of them are either expensive or use environmentally hazardous substances. Producing tiny structures or nano-arrays with unique properties that consistently outperform their bulk or single particle counterparts is the aim of nanotechnology. Novel green syntheses that are non-hazardous and reasonably priced

[5-7] have become necessary due to the growing concern about how to decrease or eliminate the usage of environmentally harmful compounds in accordance with the principles of green chemistry [4]. Deacetylating chitin naturally produces chitosan (CS), also called poly [ $\beta$ -(1  $\rightarrow$  4)-2-amino-2-deoxy-D-glucopyranose], a high molecular weight cationic cellulose biopolymer. There is a lot of chitinous stuff in this product. Chitosan (CS) is a hydrophilic, biodegradable, biocompatible, and cost-effective polymer [10–12]. Because of the strong adsorptive potential of the highly reactive amino and carboxyl groups in chitosan's molecular structure [13–15], they can be used as flocculents and adsorbents in the wastewater and water treatment industries [16–18]. Furthermore, chitosan has anti-diabetic and anti-oxidant properties [19–21]. Chitosan's adsorptive capacity, antidiabetic, and antioxidant properties can be enhanced by combining it with other metal oxide nanoparticles, especially bimetallic Ag nanoparticles. The biological method of producing nanoparticles, which is believed to be environmentally safe and a fantastic alternative to chemical and physical methods, uses plant extracts [22]. Despite the high energy and chemical requirements of physical and chemical methods and the use of proteins in biological agent manufacturing,

phytochemicals and more naturally occurring enzymes for the production of possible capping and nanohybrids [23]. Ag<sub>2</sub>ONPs, or silver nanoparticles, are produced biologically and are environmentally benign, nontoxic, simple to employ, and reliable [24]. For usage in a range of medical applications, green-synthesised Ag<sub>2</sub>ONPs are safe and biocompatible. (Ag<sub>2</sub>ONPs) diverse biological activities have resulted in their inclusion in a number of household goods, such as textiles, antiseptic spray, antibacterial agents, and wound dressing agents [25]. Because (Ag<sub>2</sub>ONPs) are useful for diagnosing, administering medications, and treating a wide range of diseases, the scientific community's knowledge of them has grown in a favourable and unprecedented way [21]. It has been found to have antibacterial, anti-diabetic, and antioxidant properties [26]. Instead of using any hazardous chemicals, the current research on the production of green nanoparticles uses biopolymers, such as chitosan, as stabilising and capping agents. Excellent among biocompatible plastics Chitosan has garnered interest due to its many benefits, such as its low toxicity and antibacterial capabilities [27]. This enables the production of larger quantities of smaller, more homogeneously formed, extremely stable, and biocompatible nanoparticles. By functionalising chitosan with metallic ions, the antibacterial activity can be enhanced due to its functional groups. It was shown that specific concentrations of metallic ions in chitosan-metal nanoparticles had antibacterial properties without causing a cytotoxic response. Additionally, using a green strategy provides a process that is sustainable, inexpensive, and ecologically friendly with a lower environmental impact [28, 29]. Diabetes is the most common disease in the world. Silver nanoparticles (Ag<sub>2</sub>ONPs) have demonstrated significant inherent anti-inflammatory, antibacterial, antiviral, and antifungal activities. The water-soluble vitamin ascorbic acid has strong antioxidant qualities, while the oligosaccharide biopolymer chitosan is great at lowering blood sugar levels [29].

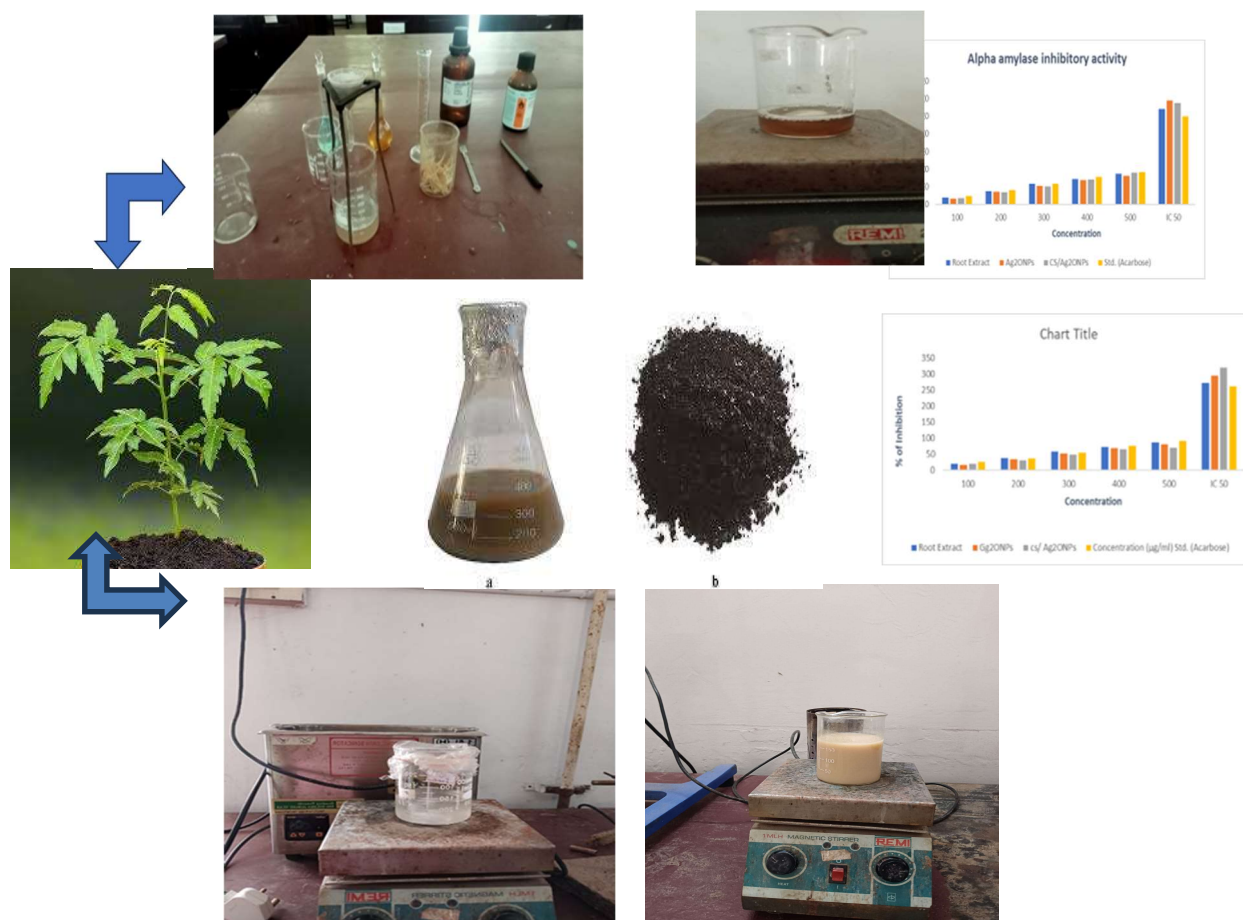


**Figure -1;** colour change yellow black colour indicate the formation of the Ag<sub>2</sub>ONPs and CS-Ag<sub>2</sub>O nanocomposite

## 2.3 Method and Materials

### 2.1 Materials

Silver nitrate (AgNO<sub>3</sub>) crystal and medium molecular weight chitosan (~400,000) were acquired from Sigma-Aldrich together with acetic acid glacial (CH<sub>3</sub>COOH) solution (99.8%). water that has been distilled.

### 2.3 Preparation of Solution

The *Azadirachta indica* root was cleaned with ordinary water and then rinsed with distilled water to create the plant extract. The root samples were allowed to air-dry for two to seven days before being processed into a fine powder with a mixer grinder. Five grammes of the powdered root and one hundred millilitres of sterile water were combined, heated to fifty degrees Celsius for half an hour, and then allowed to cool. After being filtered through Whatman filter paper, the clear extract was collected and kept at 4 °C for the next step.

### 2.3 Chitosan /Silver oxide nanocomposite preparation

0.5 g of pure CS powder was dissolved in 100 mL of 1% acetic acid. After vortexing the mixture to encourage complete dissolve, it was centrifuged for two hours at 150 rpm. After adding 0.5 g of  $\text{AgNO}_3$  salts to this mixture, it was stirred for two hours. Then, when freshly prepared *Azadirachta Indica* root extract was added dropwise to this combination, a dark-brown precipitate with gas evolution was observed. The metal salts in the liquid were totally reduced after an additional hour of stirring. The resulting black solid was cleaned three times using distilled water to get rid of impurities. The flask was coated in aluminium foil to keep light from touching it. A 40 W Tungsten was placed 5 cm from the Erlenmeyer flask. The formation of silver oxide nanoparticles was indicated by the hue changing from brown to black. The absorbance of chi-Ag NPs in four millilitres of water at 200–450 nm was measured using a UV-Vis spectrophotometer.

### 2.4 Synthesis of Silver oxide nanoparticles

In conical flasks, 80 ml of 1M  $\text{AgNO}_3$  (silver nitrate) was mixed with 20 ml of the filtered Neem root extract.  $\text{Ag}_2\text{ONPs}$  were formed when the mixture was allowed to react. Using UV-visible spectroscopy, the reaction mixture was examined for colour and absorbance changes at 30-minute intervals for five hours. The production of  $\text{Ag}_2\text{ONPs}$  was suggested by the emergence of a yellowish-black hue. The  $\text{Ag}_2\text{ONPs}$  were separated from the liquid by centrifuging the reaction mixture for 30 minutes at 10,000 rpm. Following centrifugation, the residue was frozen, and any residual moisture was subsequently lyophilised (freeze-dried) [32]. The synthesised  $\text{Ag}_2\text{ONPs}$  are present in the resultant powder, and their size, shape, and characteristics can now be further assessed using methods like XRD, EDAX, and FTIR.

## 3. Result and Discussion

### 3.1 UV- Vis spectroscopy

UV-Vis absorbance spectra were used to characterise the generated  $\text{Ag}_2\text{ONPs}$  and chitosan  $\text{Ag}_2\text{O}$  nanocomposite. A steady peak with the highest absorbance at 425 nm appeared over time, confirming that the manufacture of  $\text{Ag}_2\text{ONPs}$  using the Neem root extract was successful (Figure 3.3). The surface plasmon resonance band of the chitosan nanocomposite  $\text{Ag}_2\text{ONPs}$  is located at 450 nm. The detection of  $\text{Ag}_2\text{ONP}$  synthesis is shown by the increasing absorbance intensity.

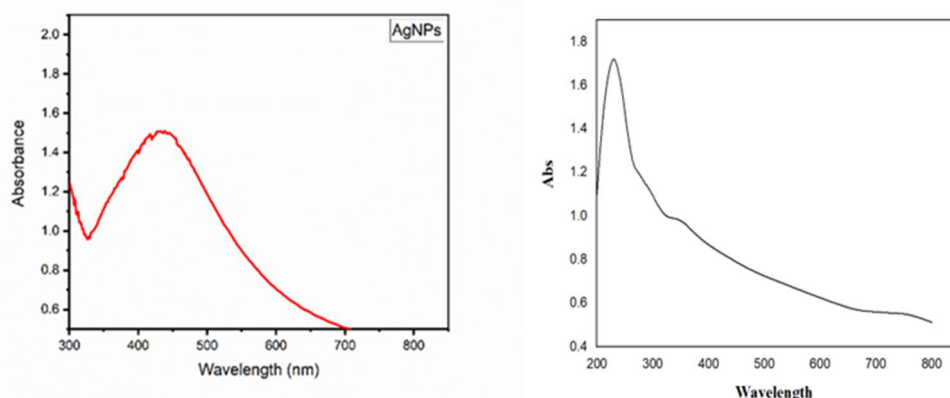


**Figure-3.3;** The UV-visible absorption spectrum of  $\text{Ag}_2\text{ONPs}$  that were biosynthesised with root extract from *A. indica*. After being incubated with 0.01 mM  $\text{AgNO}_3$  and 5 mL root extract for 30 minutes at 85 °C, the absorption spectra of  $\text{Ag}_2\text{ONPs}$  and CS/ $\text{Ag}_2\text{ONPs}$  showed a high peak at 425 nm and 450 nm.

### 3.2 FTIR Spectroscopy

The  $\text{Ag}_2\text{O}$  FTIR analysis was carried out in order to identify the possible biomolecules responsible for stabilising and capping the chitosan/ $\text{Ag}_2\text{O}$  nanocomposite and artificially generated  $\text{Ag}_2\text{ONPs}$ . The peaks at 1606  $\text{cm}^{-1}$  and 1388  $\text{cm}^{-1}$  are caused by the free C-H or N-H stretching vibration of the aromatic molecule and the bending mode C-N stretching vibration, respectively. The FTIR spectra, which showed peaks at 3784  $\text{cm}^{-1}$  O-H stretching, 3435  $\text{cm}^{-1}$  N-H stretching, 831  $\text{cm}^{-1}$ , and 588  $\text{cm}^{-1}$  attributed to silver oxide NPs vibration, validated the formation of the nanoparticles. The findings showed that the biological molecules were produced

using a green synthesis technique (Figure 3.2).

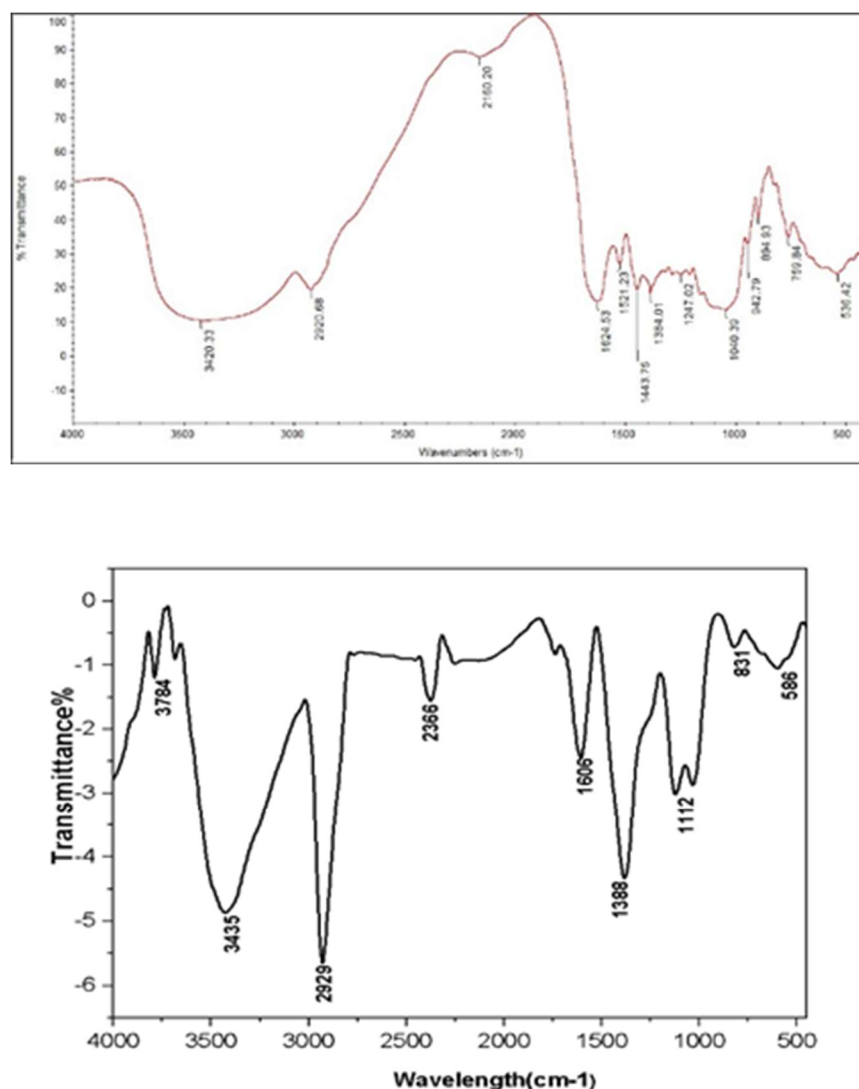


Figure -3.2; The Fourier transform infrared spectrum of the dried powder of the the biosynthesised Ag<sub>2</sub>O nanocomposite, as shown in Figure 3.1(b), was determined using the chitosan-based nanocomposite silver oxide. The chitosan nanocomposite Ag<sub>2</sub>O's spectra are represented by the strong peaks at 536.42 cm<sup>-1</sup> C-I stretching. CH stretching, the strong broad peak for absorption at 3420 cm<sup>-1</sup>, 2920 cm<sup>-1</sup>. The FTIR spectra's displacement peaks at 1040 cm<sup>-1</sup> C=S stretching and 1624.53 cm<sup>-1</sup> C=C stretching vibration verified the nanocomposite. The peaks at cm<sup>-1</sup> and 894 cm<sup>-1</sup> are caused by the bending mode C-N vibration of stretching and the free C-H or N-H stretching vibration of the aromatic molecule, respectively.

### 3.3 XRD Spectroscopy

The chitosan Ag<sub>2</sub>O nanocomposite and Ag<sub>2</sub>ONPs are crystalline, according to XRD. The diffractogram shows the intensity of the diffracted beams plotted against their diffraction angles. The spectra display the crystal planes' characteristics. At different orientations, the biogenesis of Ag<sub>2</sub>ONPs was obtained at the x-ray diffraction peaks. The Debye-Scherrer equation was used to calculate the nanoparticles' size.

$$D = k\lambda / \beta \cos\theta$$

Using X-ray reflectance (XRD) to examine synthesised silver nanoparticles from root extract, diffraction peaks

at  $2\theta = 37.8^\circ$  (310),  $37.6^\circ$  (310),  $44.16^\circ$  (510),  $66.04^\circ$ , and  $76.98^\circ$ , respectively, were used to identify the  $\text{Ag}_2\text{ONPs}$  (Figure 3.3(A)). When X-ray reflectance (XRD) was used to examine the synthesized silver nanoparticles from root extract, the CS/ $\text{Ag}_2\text{ONPs}$  were identified by diffraction peaks at  $2\theta = 14.7$  (111),  $55.85$  (510) and  $27.18$  (310) respectively Figure

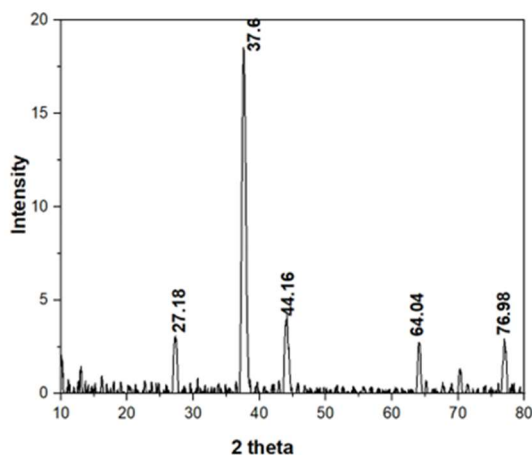


Figure-3.3;(A)

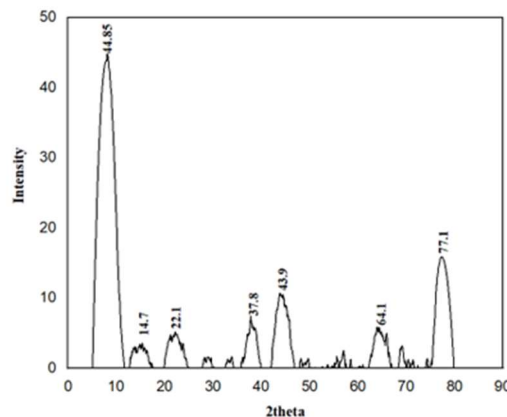


Figure-3.3 ;(b)

**Figure -3.3;** X- Ray diffraction pattern of  $\text{Ag}_2\text{ONPs}$  characteristics peak for nano silver oxide have been observed at  $2\theta = 27.18$

### 3.4 Analysis of EDAX

The synthesised CS- $\text{Ag}_2\text{O}$  NC and  $\text{Ag}_2\text{O}$  NPs were subjected to elemental analysis by EDX. EDX analysis validated the chemicals. Silver oxide peaks were seen in two different places (50.17 and 7.50) in the EDX spectra. According to Figure 3.4 (A), the proportions of oxygen, carbon, and nitrogen were 10.49, 6.13, 26.84, and 0.76, respectively. There are two different locations where the CS- $\text{Ag}_2\text{ONPs}$  peaks (63.32 and 2.09). According to Figure 3.4 (b), the proportions of oxygen, silicon, carbon, and magnesium were 1.58, 5.06, 1.74, and 0.82, respectively.

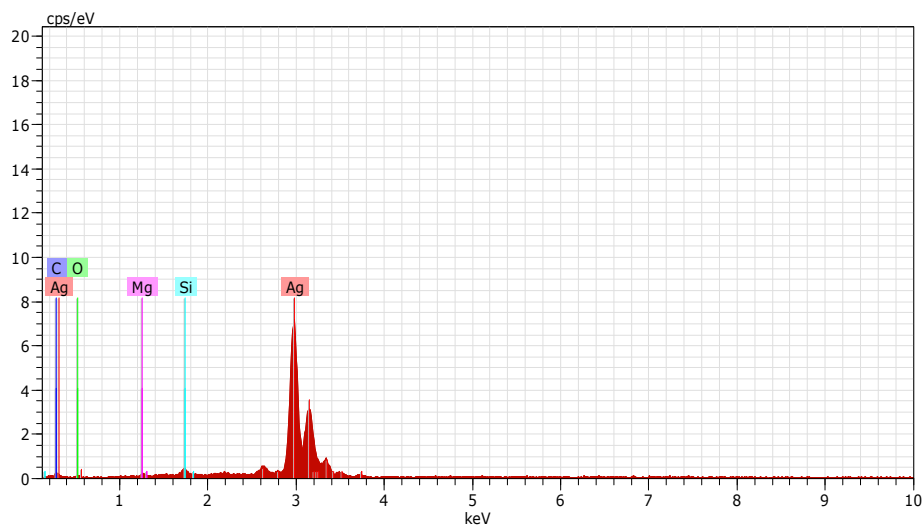
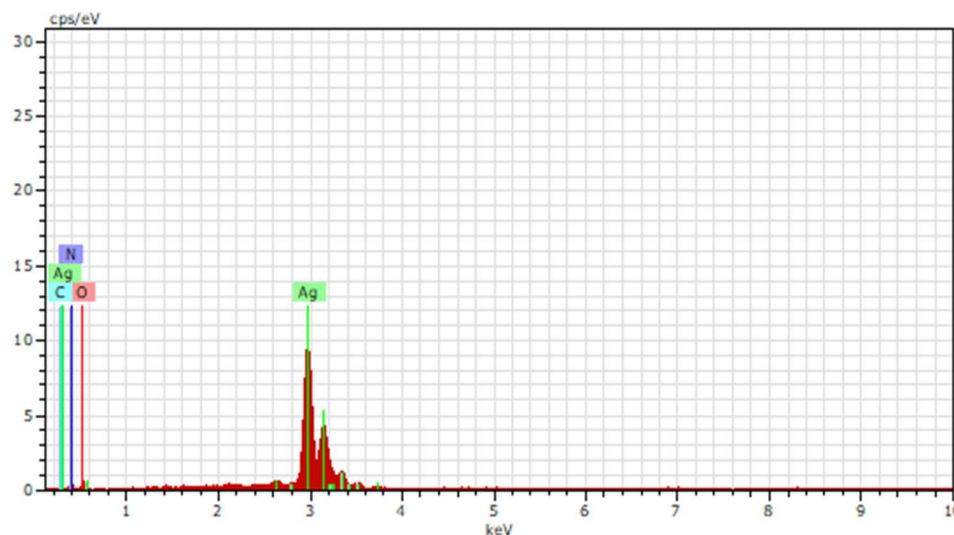


Figure-3.4 (A) The silver oxide nanoparticles EDX spectrum analysis





**Figure-;3.4 (b)** The chitosan silver oxide nanocomposite EDX spectrum analysis

#### 4. Invitro anti- diabetic activity

##### 4.1 Sample preparation

Dissolve 100 mg of the sample in 100 ml of deionised water. For the purpose of assessing the in vitro antidiabetic activity, samples and standard acarbose were generated in various concentrations (100µg/ml, 200µg/ml, 300µg/ml, 400µg/ml, and 500µg/ml) using deionised water.

##### 4.2 In vitro $\alpha$ -Amylase Inhibition Study

4.3 The liquid sample was created at different concentrations (100–500 µg/ml) after drying. The solid sample also produced the same concentration for analysis. A variety of sample concentrations, including 100 µg/ml, 200 µg/ml, 300 µg/ml, 400 µg/ml, and 500 µg/ml, were produced using phosphate buffer (pH 6.9). A 10-minute incubation period was conducted at 25°C with 500 µl of the sample and 500 µl of 20 mM phosphate buffer pH 6.9, which included 0.5 mg/ml of  $\alpha$ -amylase. After pre-incubation, 1000 µl of a 0.5% starch solution in 20 mM phosphate buffer (pH 6.9) was added. The reaction mixtures were then incubated at 25°C for 10 minutes. After pre-incubation, 1000 µl of a 0.5% starch solution in 20 mM phosphate buffer (pH 6.9) was added. The reaction mixtures were then incubated at 25°C for 10 minutes. The reaction was stopped with 500 µl of 96 mM 3, 5-dinitrosalicylic acid (DNS) colour reagent. The test tubes were incubated in a boiling bath for five minutes before being allowed to cool to room temperature.

$$\% = \frac{Ac-As}{Ac} \times 100$$

At 540 nm, absorbance (A) was measured. At 540 nm, absorbance (A) was measured. The inhibitory activity of  $\alpha$ -amylase and the percentage of inhibition were computed using acarbose as a positive control.

##### 4.4 In Vitro $\alpha$ -glucosidase inhibition Study

The  $\alpha$ -glucosidase inhibitory activity was measured using the procedure described by Apostolidis et al. [31]. To dissolve yeast  $\alpha$ -glucosidase at 0.1 U/ml, 100 mM phosphate buffer (pH 7.0) was mixed with 2000 mg/ml of bovine serum albumin and 200 mg/ml of sodium azide. Five milligrammes of  $\alpha$ -D-glucopyranoside para nitrophenyl. 50 µl of Para nitrophenyl- $\alpha$ -D-glucopyranoside solution was added to 0.1mol phosphate buffer (pH 6.9) after 100 µl of yeast  $\alpha$ -glucosidase solution and 50 µl of sample extract at different concentrations (100, 200, 300, 400, and 500 µg/ml) were incubated for 10 minutes at 25°C. The absorbance of the reacting mixture at 405 nm was measured following five minutes of incubation at 25°C, the reacting mixture's absorbance was measured at 405 nm. The following formula was utilised to determine the inhibitory activity of glucosidase, with acarbose serving as a positive control.

$$\text{of inhibition} = (\text{Control O.D.} - \text{Test O.D.}) / \text{Control O.D.} \times 100$$

100% enzyme activity is shown by control incubations, which were conducted similarly but using different extracts. To accommodate for absorbance produced by the extract, buffer solution was used in place of enzyme solution during blank incubation, and absorbance was then measured.

#### 4.5 Comparison of Silver Oxide Nanoparticles and Chitosan-Silver Oxide Nanocomposite for Anti-Diabetic Activity

Silver oxide nanoparticles (Ag<sub>2</sub>ONPs) have shown potential as anti-diabetic drugs because they can change insulin sensitivity and glucose metabolism. Chitosan, a biocompatible and biodegradable polymer, has been used to make a silver oxide nanoparticle and nanocomposite (CS-Ag<sub>2</sub>O NC). This comparison aims to evaluate and contrast the anti-diabetic qualities of Ag<sub>2</sub>O NPs and CS-Ag<sub>2</sub>O NC. Ag<sub>2</sub>ONPs and the CS-Ag<sub>2</sub>O nanocomposite showed different mechanisms of anti-diabetic effect. Ag<sub>2</sub>ONPs primarily altered glucose metabolism by increasing insulin sensitivity and glucose absorption. Alpha-glucosidase inhibition, glucose metabolism control, and antioxidant activity were all part of the more comprehensive mechanism that CS-Ag<sub>2</sub>O NC displayed. When compared to Ag<sub>2</sub>O NPs, the CS-Ag<sub>2</sub>O nanocomposite showed reduced toxicity and improved biocompatibility. The toxicity of silver oxide was reduced with the help of the chitosan matrix.

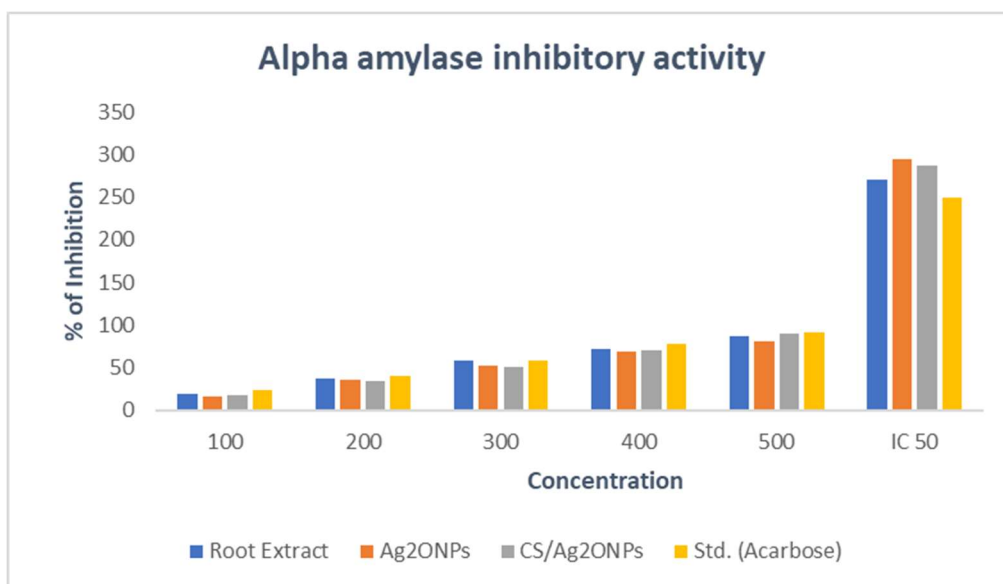


Figure-; 4.2 (A) Graphical representation of Alpha amylase activity



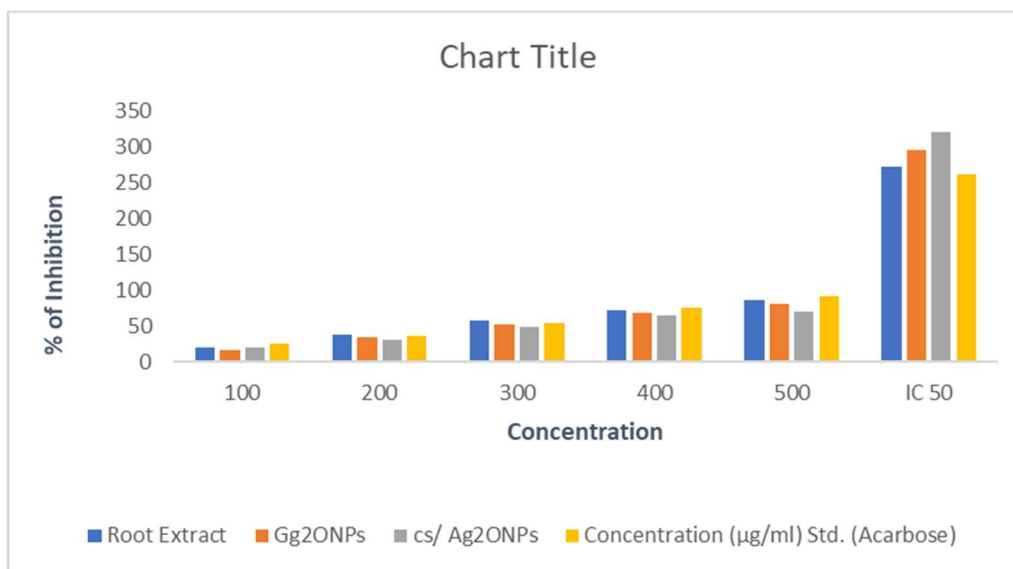


Figure-; 4.3 (b) Graphical representation of Alpha glucosidase activity

## 5. Conclusion

Traditional Indian medicine uses components of the *Azadirachta indica* tree to treat ailments. Their application in numerous industries increases the need to produce Ag<sub>2</sub>O NPs and CS-Ag<sub>2</sub>O nanocomposite on a large scale in an accessible, economical, and environmentally acceptable manner. Although the CS-Ag<sub>2</sub>O nanocomposite demonstrated a more thorough mechanism and enhanced biocompatibility, the Ag<sub>2</sub>O NPs and CS-Ag<sub>2</sub>O NC both shown anti-diabetic efficacy. A promising substance for the creation of anti-diabetic treatments could be CS-Ag<sub>2</sub>O NC. The green synthesis method is an alternative to the chemical technique. The bio-functions of biopolymers embedded in metal oxide (MO) nanoparticles are diverse. When it comes to enhancing biological activity, chitosan-incorporated MOs are an interesting class of support matrices. Chitosan-incorporated MOs are an interesting class of support matrices for enhancing biological function when compared to other support matrices. *Azadirachta indica* root extract of Ag<sub>2</sub>ONPs and chitosan based on nanocomposite has demonstrated anti-diabetic properties and is a good option in both industrial and medical applications.

## Reference

1. G. Zhang, D.J. Wang, Fabrication of heterogeneous binary arrays of nanoparticles via colloidal lithography, J. Am. Chem. Soc. 130 (2008) 5616–5617, <https://doi.org/10.1021/ja710771j>.
2. [2] F. Mafune, J. Kohno, Y. Takeda, T.J. Kondow, Full physical preparation of size- selected gold nanoparticles in solution: Laser Ablation and Laser-Induced Size Control, J. Phys. Chem. B 106 (2002) 7575–7577, <https://doi.org/10.1021/jp020577y>.
3. [3] P.T. Anastas, M.M. Kirchhoff, Origins, current status, and future challenges of green chemistry, Acc. Chem. Res. 35 (2002) 686–694, <https://doi.org/10.1021/ar010065m>.
4. [4] P. Mohanpuria, N.K. Rana, S.K. Yadav, Biosynthesis of nanoparticles: technological concepts and future applications, J. Nanopart. Res. 10 (2008) 507–517, <https://doi.org/10.1007/s11051-007-9275-x>.
5. [5] M. Pattanayak, P.L. Nayak, Green synthesis and characterization of zero valent iron nanoparticles from the leaf extract of *Azadirachta indica* (neem), World J Nano Sci Tech 2 (2013) 6–9, <https://doi.org/10.5829/idosi.wjnst.2013.2.1.21132>.

6. [6] A.A. Olajire, A. Kareem, A. Olaleke, Green synthesis of bimetallic Pt@Cu nanostructures for catalytic oxidative desulfurization of model oil, *J Nanostruct Chem* 7 (2017) 159–170, <https://doi.org/10.1007/s40097-017-0223-8>.
7. [7] A.A. Olajire, N.F. Ifediora, M.D. Bello, N.U. Benson, Green synthesis of copper nanoparticles using *Alchornea laxiflora* leaf extract and their catalytic application for oxidative desulphurization of model oil, *Iran J Sci Technol Trans Sci* 42 (4) (2018) 1935–1946, <https://doi.org/10.1007/s40995-017-0404-9>.
8. N.R. Kim, K. Shin, I. Jung, M. Shim, M. Lee, Ag-Cu bimetallic nanoparticles with enhanced resistance to oxidation: a combined experimental and theoretical study, *J. Phys. Chem. C* 118 (2014) 26324–26331, <https://doi.org/10.1021/jp506069c>.
9. J. Sopoušek, J. Pinkas, P. Brož, J. Buršík, V. Vykoukal, D. Škoda, A. Stýskalík, O. Zobač, J. Vřeštitel, A. Hrdlička, J. Šimbera, Ag-Cu colloid synthesis: bimetallic nanoparticle characterization and thermal treatment, *J. Nanomater.* 2014 (2014). <https://doi.org/10.1155/2014/638964>.
10. G. Crini, P.M. Badot, Application of chitosan, a natural aminopolysaccharide, for dye removal from aqueous solutions by adsorption processes using batch studies: a review of recent literature, *Prog. Polym. Sci.* 33 (2008) 399–447, <https://doi.org/10.1016/j.progpolymsci.2007.11.001>.
11. E.Y. Ozmen, M. Sezgin, A. Yilmaz, M. Yilmaz, Synthesis of  $\beta$ -cyclodextrin and starch based polymers for sorption of azo dyes from aqueous solutions, *Bioresour. Technol.* 99 (2008) 526–531, <https://doi.org/10.1016/j.biortech.2007.01.023>.
12. B.J. Liu, D.F. Wang, Y. Xu, G.Q. Huang, Adsorption properties of Cd(II)-imprinted chitosan resin, *J. Mater. Sci.* 46 (2011) 1535–1541, <https://doi.org/10.1007/s10853-010-4958-6>.
13. N.W.S. Wan, N.F.M. Ariff, M.A.K.M. Hanafiah, Preparation, characterization, and environmental application of crosslinked chitosan coated bentonite for tartrazine adsorption from aqueous solutions, *Water Air Soil Pollut.* 206 (2010) 225–236, <https://doi.org/10.1007/s11270-009-0098-5>.
14. K.M. Gregorio-Jauregui, M.G. Pineda, J.E. Rivera-Salinas, G. Hurtado, H. Saade, J.L. Martinez, A. Ilyina, R.G. Lopez, One-step method for preparation of magnetic nanoparticles coated with chitosan, *J. Nanomater.* 2012 (2012) 1–8, <https://doi.org/10.1155/2012/813958>.
15. L. Fan, Y. Zhang, C. Luo, H. Qiu, M. Sun, Synthesis and characterization of magnetic  $\beta$ -cyclodextrin–chitosan nanoparticles as nano-adsorbents for removal of methyl blue, *Int. J. Biol. Macromol.* 50 (2012) 444–450, <https://doi.org/10.1016/j.ijbiomac.2011.12.016>.
16. A. Kangama, D. Zeng, X. Tian, J. Fang, Application of chitosan composite flocculant in tap water treatment, *J. Chem.* 2018 (2018) 9, <https://doi.org/10.1155/2018/2768474>.
17. J.J. Fera-Diaz, M.J. Tavera-Quiroz, O. Vergara-Suarez, Efficiency of chitosan as a coagulant for wastewater from slaughterhouses, *Indian J. Sci. Technol.* 11 (3) (2018), <https://doi.org/10.17485/ijst/2018/v11i3/117169>.
18. H.A. Abdullah, A.J. Jael, Chitosan as a widely used coagulant to reduce turbidity and color of model textile wastewater containing an anionic dye (Acid blue), *IOP Conf. Ser. Mater. Sci. Eng.* 584 (2019), 012036 IOP Publishing, <https://doi.org/10.1088/1757-899X/584/1/012036>.
19. D.R. Ting, Y. Shen, Antibacterial finishing with chitosan derivatives and their nanoparticles, *Dye. Finish.* 14 (2005) 12–14.
20. P. Gupta, M. Bajpai, S.K. Bajpai, Investigation of antibacterial properties of silver nanoparticle-loaded poly (acrylamide-coitaconic acid)-grafted cotton fabric, *J. Cotton Sci.* 12 (2008) 280–286.
21. J. An, Q. Luo, X. Yuan, D. Wang, X. Li, Preparation and characterization of silver–chitosan nanocomposite particles with antimicrobial activity, *J. Appl. Polym. Sci.* 120 (2011) 3180–3189, <https://doi.org/10.1002/app.33532>.
22. M. Govindappa, B. Hemashekhar, M.-K. Arthikala, R.V. Ravishankar, Y.L. Ramachandra, Characterization, antibacterial, antioxidant, antidiabetic, anti inflammatory and antityrosinase activity of green synthesized silver nanoparticles using *Calophyllum tomentosum* leaves extract, *Results Phys* 9 (2018) 400–408.
23. B. Nair, T. Pradeep, Coalescence of nanoclusters and formation of submicron crystallites assisted by *Lactobacillus* strains, *Growth Des* 2 (2002) 293–298.

24. K.B. Narayanan, N. Sakthivel, Biological synthesis of metal nanoparticles by microbes, *Adv. Colloid Interface Sci.* 156 (2010) 1–13.
25. K. Chaloupka, Y. Malam, A.M. Seifalian, Nanosilver as a new generation of nanoparticle in biomedical applications, *Trends Biotechnol.* 28 (2010) 580–588.
26. G. Das, J.K. Patra, T. Debnath, A. Ansari, H.-S. Shin, Investigation of antioxidant, antibacterial, antidiabetic, and cytotoxicity potential of silver nanoparticles synthesized using the outer peel extract of *Ananas comosus* (L.), *PloS One* 14 (2019), e0220950.
27. Adlim, M., Khaldun, I., Hanum, L., Arsha, R., Nadia, Y., SyahliDayani, S., 2020. Properties of slow-release magnesium and calcium nitrate tablets composed of rice- husk-ash with chitosan coating, within water and in several types of soil. *J. Phys. Conf. Ser.* 1529, 032085 <https://doi.org/10.1088/1742-6596/1529/3/032085>.
28. Adlim, M., Ramayani, R.F.I., Khaldun, I., Muzdalifah, F., Sufardi, S., Rahmaddiansyah, R., 2021b. Fertilizing properties of urea-magnesium slow-release fertilizer made of rice-husk-ash natural-rubber chitosan composite. *Rasayan J. Chem.* 14, 1851–1859. <https://doi.org/10.31788/RJC.2021.1436091>.
29. Adil, S.F., Assal, M.E., Khan, M., Al-Warthan, A., Siddiqui, M.R.H., Liz-Marz' an, L.M., 2015. Biogenic synthesis of metallic nanoparticles and prospects toward green chemistry. *Dalt. Trans.* 44, 9709–9717. <https://doi.org/10.1039/c4dt03222e>.
30. Apostolidis, E., Kwon, Y. I., & Shetty, K. (2007). Inhibitory potential of herb, fruit, and fungal-enriched cheese against key enzymes linked to type 2 diabetes and hypertension. *Innovative Food Science & Emerging Technologies*, 8(1), 46-54.
31. Alqahtani A.S., Hidayathulla S., Rehman M.T., ElGamal A.A., Al-Massarani S., Razmovski-Naumovski V., Alqahtani M.S., El Dib R.A., AlAjmi M.F. Alpha-Amylase and Alpha-Glucosidase Enzyme Inhibition and Antioxidant Potential of 3-Oxolupenal and Katonic Acid Isolated from *Nuxia oppositifolia*. *Biomolecules*. 2019;10: 61.

